JOURNAL OF MATERIALS SCIENCE 26 (1991) 5799–5805

Microstructures and Vickers hardness of rapidly solidified Al–Cu alloys near the Al–Al_2Cu equilibrium eutectic composition

YIBIN ZHANG, TOSHIMI YAMANE, KEIICHI HIRAO, YORITOSHI MINAMINO
Department of Materials Science and Engineering, Faculty of Engineering, Osaka University, Yamadaoka, Suita 565, Japan

Al–Cu alloys near the Al–Al_2Cu equilibrium eutectic composition were rapidly solidified by the single-roller method. Two-zone structures were observed in transverse sections of Al–24.8, 30.0, 32.7, 33.2, 37.0 and 40.3 mass % Cu alloy ribbons, which were interpreted on the basis of the difference in cooling rates and of the temperature gradients between the chilled and free-surface sides of the ribbons. Non-equilibrium eutectic structures, cellular and irregular lamellar, were seen at the chilled side because the alloy liquids were directionally solidified with coupled eutectic growth. The coupled zone of the Al–Cu alloy expanded over the composition range 24.8–40.3 mass % Cu by rapid solidification. Dendritic structures were formed at the unchilled side of Al–24.8, 30.0, 37.0 and 40.3 mass % Cu alloys. Vickers hardness values at the chilled side differed from those at the unchilled side due to the difference in the microstructure.

1. Introduction

In general, the Al–Cu alloy of the Al–Al_2Cu eutectic composition can be solidified with three different eutectic microstructures, cellular, lamellar and degenerate, depending on the growth velocity, and the temperature gradient near the interface between the liquid and solid [1, 2]. In non-equilibrium solidification, a eutectic structure without primary crystals is produced over the range of conditions (generally composition and undercooling values) called "the coupled zone". The coupled zone of the Al–Cu system was reported previously in the composition range 25.0–36.0 mass % Cu with a temperature gradient of $G = 185\ \mathrm{K\,cm^{-1}}$ and a growth velocity of $V = 1.6 \times 10^{-4}\ \mathrm{cm\,s^{-1}}$ [3–5]. Using the method of rapid solidification, the Al–Cu alloy of eutectic composition forms an amorphous phase at a cooling rate faster than $10^9\ \mathrm{K\,s^{-1}}$ [6], and special structures, which are parallel alternate lamellar, degenerate eutectic, cellular and fine periodic, are obtained at a cooling rate of 10^5–$10^8\ \mathrm{K\,s^{-1}}$ [7, 8]. Using the powder droplet emulsion technique, the coupled zone of the Al–Cu alloy spreads over the composition range 27.5–40.4 mass % Cu [9].

Only a few studies have attempted to explain why the non-equilibrium eutectic structure is formed under the conditions in the rapid solidification methods of powder droplet emulsion, melt spun and laser surface melting [9, 10]. However, there are no data indicating that the non-equilibrium eutectic structure is formed over a wider range of compositions of the Al–Cu alloy by the single-roller method. In a previous paper [11], the Vickers hardness of the non-equilibrium eutectic structure of rapidly solidified Al–24.8 mass % Cu alloy was measured.

The purposes of the present work were to investigate the microstructures and Vickers hardness of ribbons of rapidly solidified Al–Cu alloys near the equilibrium eutectic composition by the single-roller method, and to discuss the formation of the non-equilibrium eutectic structure in terms of the coupled zone, and the relation between the microstructure and Vickers hardness.

2. Experimental procedure

Pure (99.993 mass %) aluminium and pure (99.99 mass %) copper were melted to prepare six alloys containing 24.8, 30.0, 32.7, 33.2, 37.0 and 40.3 mass % Cu. These melt alloys at about 1000 K were rapidly solidified to ribbons of 35–200 μm thick and 5–10 mm wide on a copper roller. The diameter of the copper roller was 153 mm and the surface velocity of the roller was $13.6\ \mathrm{m\,s^{-1}}$. This single roller method is generally considered to produce cooling rates of 10^5–$10^6\ \mathrm{K\,s^{-1}}$ for ribbons of 30 μm thick [8].

X-ray diffraction spectra were measured at the chilled surface of ribbons using an X-ray diffractometer with CuK_α and a nickel filter at 40 kV and 30 mA to identify the phase.

After electrolytic etching with Keller's reagent, metallographic examination was performed on longitudinal and transverse cross-sections using optical and scanning electron microscopes. Using the optical microscope, the secondary dendrite arm spacing of

0022–2461/91 $03.00 + .12

small dendrites was determined in ribbons of non-eutectic composition alloys.

The Vickers hardness values were obtained at a load of 100 g on transverse cross-sections of ribbons as-solidified and annealed for 3.6 ks at 373, 423, 533, 588, 673 and 773 K.

3. Results

Fig. 1 shows the X-ray diffraction spectrum of the rapidly solidified Al–24.8 mass % Cu alloy. The diffraction spectrum indicates that this Al–Cu alloy has two phases, α-Al and θ-Al_2Cu.

Fig. 2 shows optical micrographs of Al–24.8, 30.0, 33.2, 37.0 and 40.3 mass % Cu alloys in the transverse cross-sections of ribbons. Two-zone microstructures are clearly found. In ribbons of the non-eutectic composition alloys, a fine structure is found at the chilled side and a dendrite structure at the unchilled side. The fine structure is etch-sensitive in hypoeutectic alloys of Al–24.8 and 30.0 mass % Cu, but not in hyper-eutectic alloys of Al–37.0 and 40.3 mass % Cu. Between the fine and dendrite microstructures there are the distinct boundaries, such as in Fig. 2b, and an indistinct border through a transitional region, as shown in Fig. 2e. The fine microstructure gradually develops into the coarse microstructure such as shown in Fig. 2a and d. The fine microstructure radiates from the chilled surface towards the unchilled side of ribbons. In ribbons of the eutectic composition alloy, as shown in Fig. 2c, the fine microstructure is found over the whole transverse cross-section; radial fine microstructure is seen at the chilled side, and clusters of fine microstructure are found at the unchilled side. There are no dendrites, but the radial fine microstructure extends over the whole transverse cross-section of thin ribbons which are less than 40–60 μm thick for the Al–30.0, 32.7 and 37.0 mass % Cu alloys of the non-eutectic composition.

On longitudinal cross-sections of ribbons, fine microstructures appear as parallel line structures for Al–24.8, 30.0, 37.0 and 40.3 mass % Cu alloys, whose line directions are approximately at $(77–85) \times \pi/180$ radians to the chilled surfaces of ribbons.

In the non-eutectic Al–Cu alloys, the dendrite structures exist at the unchilled side of ribbons. In the hypoeutectic alloys, the dendrite is the primary α-Al phase, and in the hyper-eutectic alloys, it is the primary θ-Al_2Cu phase. These dendrites have the secondary arm spacing, λ_{min}, of small dendrites near the fine microstructure region or in the transitional region. Fig. 3 shows that the secondary arm spacing of small dendrites varies with the copper concentration. λ_{min} has the largest value near the equilibrium eutectic composition

Fig. 4a–c show the SEM microstructures of Al–30.0, 32.7 and 40.3 mass % Cu alloys, respectively. At the chilled side, irregular lamellar and microcellular structures are found, the finer cellular structures occurring with increasing copper content. These solidification structures are characteristic of rapid cooling rates [3, 4, 8]. Fig. 4b shows a distinct border between the cellular structure and the lamellar structure, which is similar to the optical micrograph of Fig. 2b. Fig. 4a and c show the transitional region of the irregular lamellar region between the fine cellular structure and lamellar one. The interlamellar spacings near the cellular structure in Fig. 4a–c are 0.13–0.15 μm.

Fig. 4d shows the SEM microstructure of the border between the fine eutectic cellular and dendrite plus lamellar structures in the Al–37.0 mass % Cu alloy. This is the transitional region from the fine lamellar to the coarse lamellar structure. It clearly shows that the cellular structure at the chilled side changes to the lamellar one at the unchilled side.

The dendrite and fine cellular structures of the Al–40.3 mass % Cu alloy are shown in Fig. 4e and f. No clear boundary is observed in Fig. 4e, but in some parts a distinct border exists between the dendrite structure and the fine cellular structure regions as shown in Fig. 4f.

Fig. 5 shows Vickers hardness at the chilled and unchilled sides on a transverse cross-section of ribbons. In the hypoeutectic alloys, Vickers hardness in the fine structure of the chilled side is lower than that in the dendrite plus lamellar structures of the unchilled side. In the eutectic alloy, the ribbons have the same Vickers hardness at both sides. While in hyper-eutectic alloys, Vickers hardness in the fine structure of the chilled side is higher than that in the dendrite plus lamellar structure of the unchilled side.

Fig. 6 illustrates the relation between the Vickers hardness and the annealing temperature in Al–30.0, 33.2, 37.0 and 40.3 mass % Cu alloy ribbons. The maximum hardness is obtained in the alloys annealed at about 373–473 K for 3.6 ks, and the Vickers hardness of both sides becomes the same after annealing at higher temperature.

Fig. 7 shows an optical micrograph of Al–40.3 mass %Cu alloy ribbon annealed at 773 K for 3.6 ks. The homogeneous microstructure of α-Al and θ-Al_2Cu phases is seen on both sides of ribbon, i.e. the degeneration and coarse structures of fine cellular eutectic and dendrite plus lamellar structures on the transverse section of the ribbons.

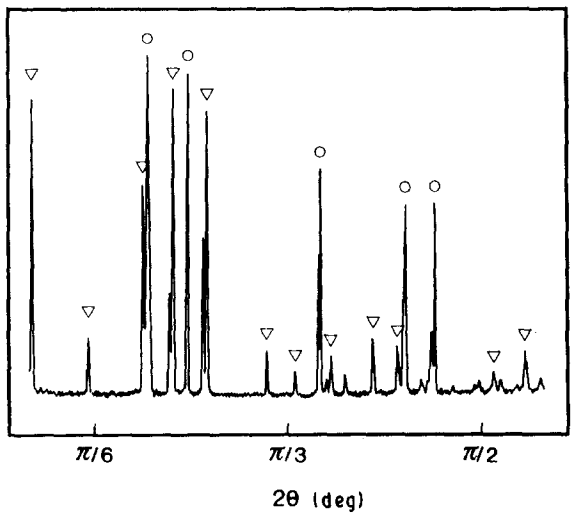

Figure 1 X-ray diffraction spectrum of rapidly solidified Al–24.8 mass % Cu alloy. (▽) θ-Al_2Cu, (○) α-Al phases.

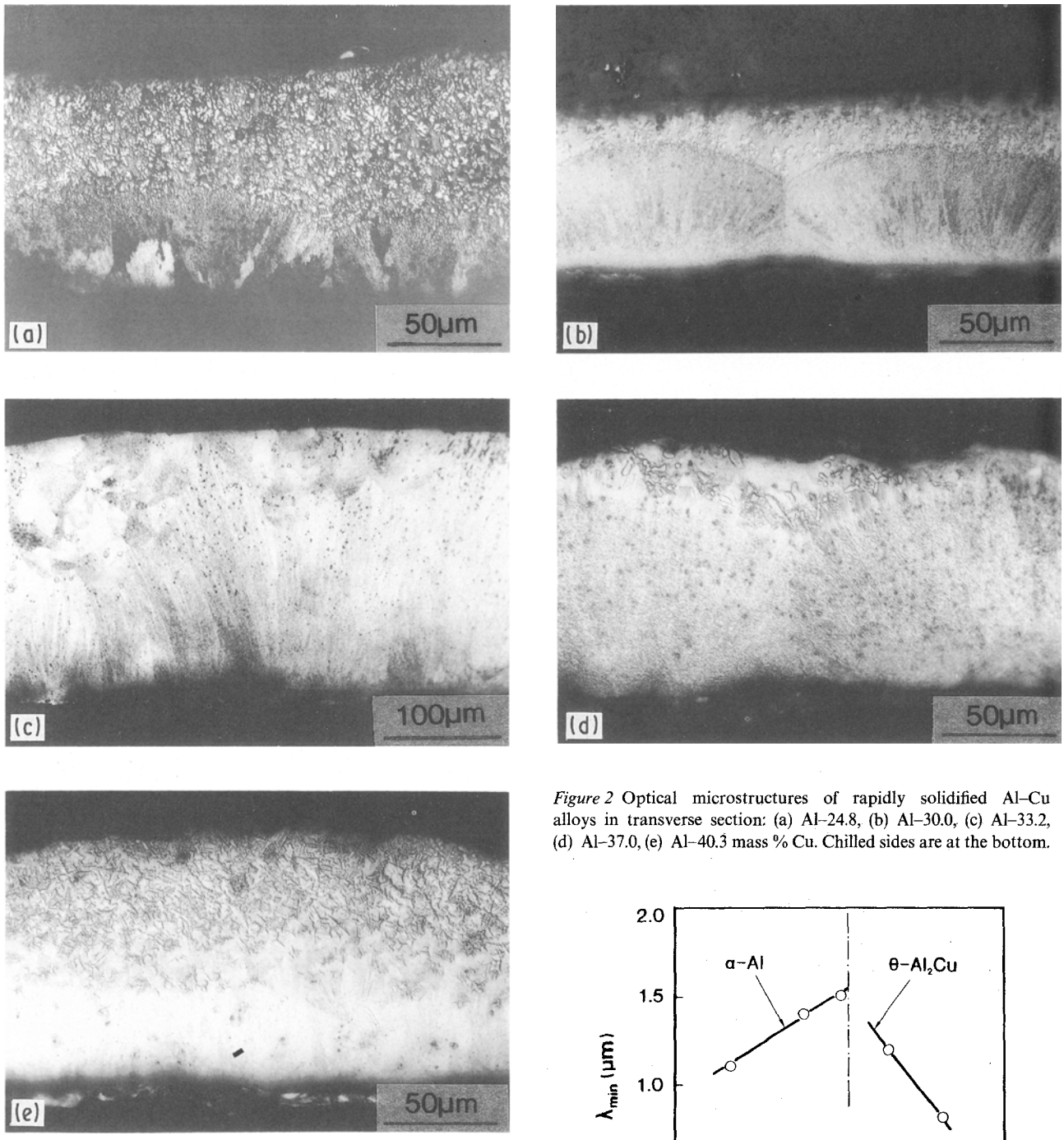

Figure 2 Optical microstructures of rapidly solidified Al–Cu alloys in transverse section: (a) Al–24.8, (b) Al–30.0, (c) Al–33.2, (d) Al–37.0, (e) Al–40.3 mass % Cu. Chilled sides are at the bottom.

Figure 3 Variation of the secondary arm spacing of minimum dendrites in rapidly solidified ribbons with copper concentration of the Al–Cu alloys.

4. Discussion

4.1. Formation of non-equilibrium eutectic and dendrite structures in the rapidly solidified Al–Cu alloys

Fig. 8 shows the formation of non-equilibrium eutectic and dendrite structures in a longitudinal cross-section of a ribbon of the non-eutectic composition Al–Cu alloys. The alloy liquid of the chilled side is directionally solidified with a rapid cooling rate and a large temperature gradient, the radial eutectic structure without primary crystals is formed by the non-equilibrium eutectic growth of the α-Al and the θ-Al_2Cu in Al–Cu alloys near the equilibrium eutectic composition. Owing to the latent heat release, the temperature gradient and the direction of solidification are changed at the unchilled side. Next to the solidified zone, first the primary dendrite, and then the lamellar eutectic structure are formed at a rapid cooling rate. Therefore, using the single-roller method, rapid solidification will result in two-zone structures in the transverse section of Al–24.8, 30.0, 37.0 and 40.3 mass % Cu alloy ribbons.

In the Al–33.2 mass % Cu alloy of equilibrium eutectic composition, no primary dendrites are formed,

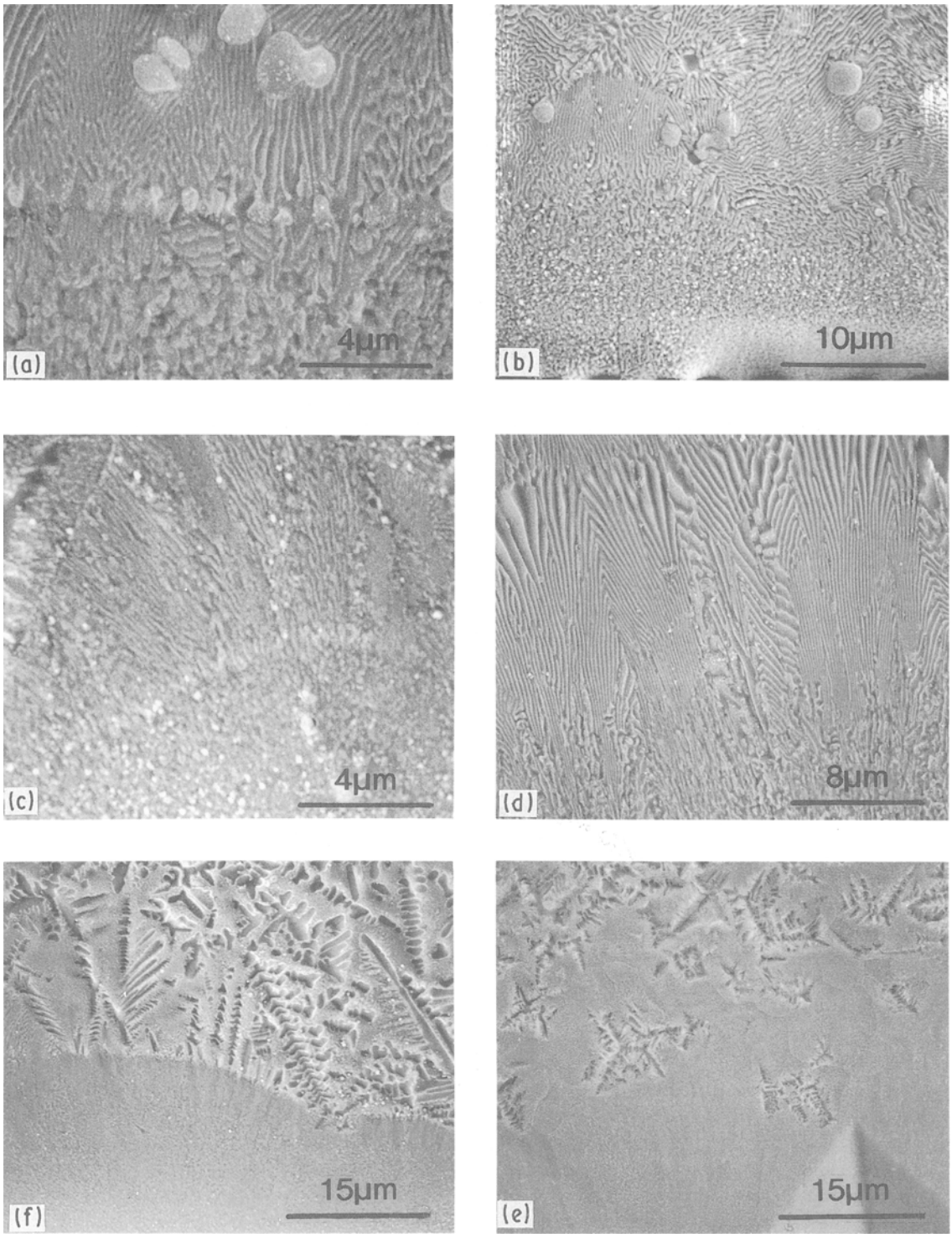

Figure 4 Scanning electron micrographs in the transverse section of rapidly solidified ribbons: (a) Al–30.0, (b) Al–32.7, (c) Al–40.3, (d) Al–37.0, (e) Al–40.3, (f) Al–40.3 mass % Cu. Chilled sides are at the bottom.

but the fine cluster microstructure is found because the temperature gradient, and the direction of solidification, are changed at the unchilled side of ribbons. When thin ribbons are produced, the whole liquid film is directionally solidified at rapid cooling rates and large temperature gradients. Obviously, the dendritic structure will not be formed in thin ribbons of non-eutectic composition alloy.

Although the cooling rate of the chilled side of the ribbons cannot be accurately measured and calculated, we can, however, evaluate the cooling rate of the unchilled side. Using the calculation method given by Matyia *et al.* [12] and λ_{min} of α-Al and θ-Al_2Cu as shown in Fig. 3, the cooling rate of the unchilled side is found to be $(0.5–2) \times 10^5$ K s^{-1}. The cooling rate of the chilled side is undoubtedly faster than this. With the calculation method provided by Adam [13], and using the liquidus temperature, eutectic temperature and thickness of the ribbons, a temperature gradient of $10^2–10^4$ K mm^{-1} is estimated in rapidly solidified ribbons. The temperature gradient and cooling rate are greater than those of normal directionally solidified ribbons, therefore, the composition region of the coupled zone will be enlarged by rapid solidification.

Under the conditions of the present experiment, it is considered that the coupled zone of the Al–Cu alloy is enlarged to encompass contents of at least 24.8–40.3 mass % Cu.

4.2. The growth velocity of non-equilibrium eutectic structures and primary dendrites

When the non-equilibrium eutectic structure is formed on a roller, the moving velocity of the liquid–solid interface V_i, is the resultant velocity of the growth velocity of non-equilibrium eutectic structures, V_{ne}, and the surface velocity of roller, V_s, as follows

$$V_i = V_{ne} + V_s \quad (1)$$

V_{ne} can be related to V_s by

$$V_{ne} = V_s \tan \phi \quad (2)$$

where ϕ is the angle between the interface growth direction and the chilled surface of ribbons. It is evident that ϕ is the angle between the parallel line of fine microstructure and the chilled surface on the longitudinal cross-section of the ribbons. From the calculation using Equation 2, it is concluded that the growth velocity of the non-equilibrium eutectic structure exceeds 60 m s^{-1}.

For the stable growth of the regular eutectic lamellar structure, the generally accepted relation [13] is

$$\lambda_e^2 V = A \quad (3)$$

where λ_e is the average eutectic lamellar spacing and V is the growth velocity of eutectic lamellar, and the constant A is equal to 108 μm^3 s^{-1} for the Al–Cu alloy system [14]. With this relation and $V_{ne} = 60$ m s^{-1}, the eutectic lamellar spacing at the chilled side should be 4×10^{-7} μm. In Al–Cu alloys of non-eutectic composition, such fine lamellar structure does not appear; only the irregular lamellar structure in the transitional region and cellular structure are observed. It is impossible for the non-equilibrium eutectic structure to be solidified to the fine regular lamellar structure with a rapid growth velocity.

As shown in Fig. 3, in Al–Cu alloys of non-eutectic composition, the secondary dendrite arm spacings of

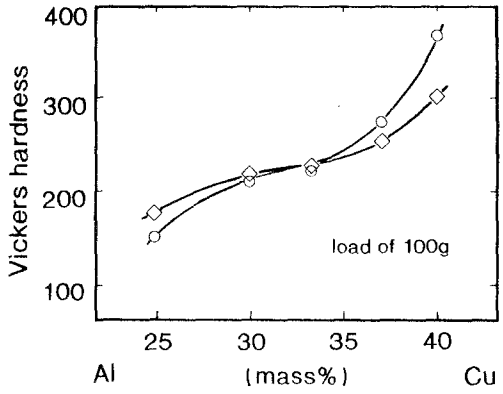

Figure 5 The relation between the Vickers hardness of rapidly solidified ribbon and copper concentration. (◇) Unchilled side, (○) Chilled side.

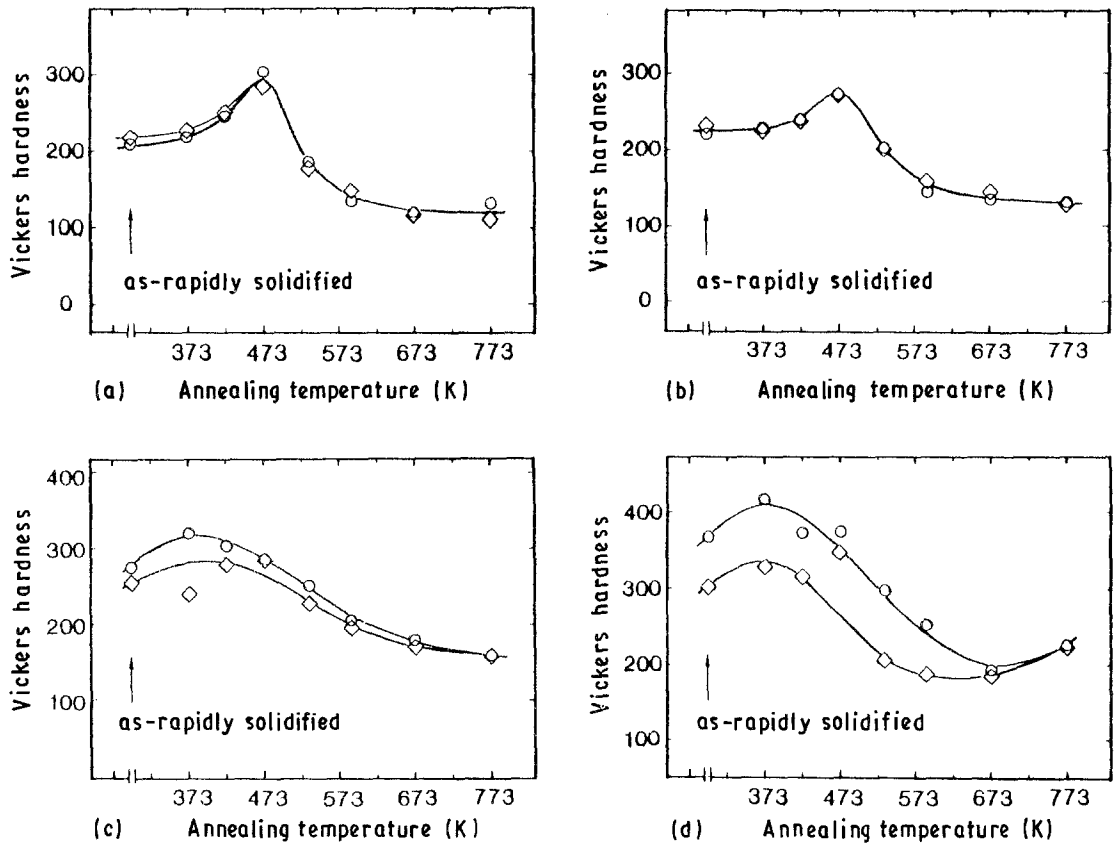

Figure 6 The relation between the Vickers hardness and the annealing temperature of rapidly solidified ribbons: (a) Al–30.0, (b) Al–33.2, (c) Al–37.0, (d) Al–40.3 mass % Cu. (◇) Unchilled side, (○) chilled side.

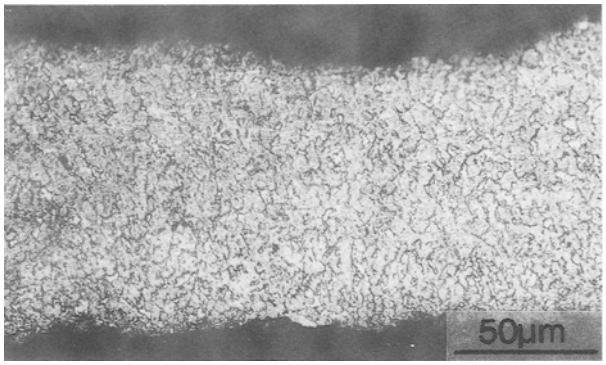

Figure 7 Optical micrograph of Al–40.3 mass % Cu alloy rapidly solidified after annealing at 773 K for 3.6 ks on transverse section of ribbon. Chilled side is at the bottom.

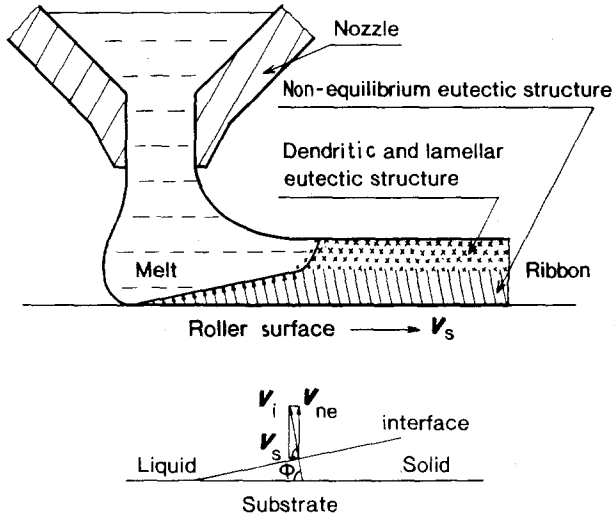

Figure 8 Schematic diagram of the rapidly solidified ribbon on a roller. The two-zone structures of non-equilibrium eutectic and dendrites plus lamellae are formed in non-eutectic composition Al–Cu alloys. V_{ne} is the growth velocity of non-equilibrium eutectic structure, V_s is the surface velocity of roller, and V_i is the moving velocity of liquid–solid interface.

small dendrites are shorter as copper concentrations become further from the equilibrium eutectic composition. It is possible that a small dendrite is formed with a critical cooling rate which is determined by the copper concentration; if the alloy composition is far from the equilibrium eutectic point, the critical cooling rate might be more rapid, and the secondary dendrite arm spacings may be decreased because the effective time of solute diffusion becomes shorter during the formation of small dendrites.

At the unchilled side, the secondary dendrite arm spacings are seven to ten times the eutectic interlamellar spacing. Generally, secondary dendrite arm spacings are some ten times the eutectic interphase spacing in the non-eutectic alloys [3]. The evaluation of cooling rates from secondary dendrite arm spacings or lamellar spacings at the unchilled side of ribbons, agree with the general values.

4.3. Vickers hardness of non-equilibrium eutectic and dendrite structures

The relation between Vickers hardness and annealing temperature of the rapidly solidified Al–24.8 mass % Cu alloy ribbons was reported previously [11]. It is indicated that the Vickers hardness of the chilled side differs from that of the unchilled side of non-eutectic composition alloys in this and in previous papers. This is due to the difference in microstructure at both sides of rapidly solidified ribbons. After annealing at high temperatures, the values of Vickers hardness at the chilled and unchilled side become equal, as a result of the degeneration and coarseness of the fine structures.

Because of the fine structures, the Vickers hardness of the cellular structure at the chilled side is higher than that of the dendritic structure region of the unchilled side of Al–Cu hypereutectic alloys, but the opposite result, which is obtained in Al–Cu hypoeutectic alloys, cannot be explained clearly. After annealing, because of the precipitation in supersaturated α-Al phase, the maximum hardness appeared in the temperature range 373–473 K.

5. Conclusions

1. The Al–Cu alloys are rapidly solidified with the non-equilibrium eutectic structure of the α-Al and θ-Al_2Cu at the chilled side of the ribbons. The coupled zone of the Al–Cu alloy is expanded by rapid solidification. The non-equilibrium eutectic structures of the chilled side are cellular and irregular lamellar structures. Dendritic structures are formed at the unchilled side of ribbons in the non-eutectic composition alloys.

2. The growth velocity of the non-equilibrium eutectic structure at the chilled side exceeds 60 m s^{-1}. At the unchilled side, secondary dendrite arm spacings of small dendrites become larger as the copper concentration approaches the eutectic composition.

3. Because different structures are formed on both sides of the rapidly solidified ribbons, Vickers hardness of the chilled side is different from that of the other side. In the hyper-eutectic alloys, the Vickers hardness of the non-equilibrium eutectic structures on the chilled side is higher than that of the dendrite structures on the other side; conversely, the Vickers hardness of the non-equilibrium eutectic structures is lower than that of the dendrite structures in the hypoeutectic alloys.

Acknowledgement

This research was financially supported by Light Metal Educational Foundation, Inc., Japan.

References

1. G. A. CHADWICK, *J. Inst. Metals* **91** (1962–63) 169.
2. *Idem, ibid.* **92** (1963–64) 18.
3. W. KURZ and D. J. FISHER, *Int. Met. Rev.* **5, 6** (1976) 177.
4. R. ELLIOT, in "Eutectic solidification Processing Crystalline and Glassy alloy", edited by M. Ashby *et al.* (Butterworths, London 1981) pp. 29, 133, 284.
5. R. M. JORDAN and J. D. HUNT, *J. Crystal Growth* **11** (1971) 141.
6. H. A. DAVIES and J. B. HULL, *J. Mater. Sci.* **9** (1974) 707.
7. D. B. WILLIAMS and J. W. EDINGTON, *ibid.* **12** (1977) 126.

8. A. KAMIO, H. TEZUKA, T. SATO, THAN TRONG LONG and T. TAKAHASHI, *J. Jpn. Inst. Light Metals* **35** (1985) 275 (in Japanese).
9. B. A. MUELLER and J. H. PEREPEZKO, *Met. Sci. Engng* **98** (1988) 153.
10. F. C. GRENSING and H. L. FRASER, *ibid.* **98** (1988) 313.
11. Y. ZHANG, T. YAMANE, K. HIRAO, *J. Jpn. Inst. Light Metals* **40** (1990) 337 (in Japanese).
12. H. MATYIA, B. C. GIESSEN, and N. J. GRANT, *J. Inst. Metals* **96** (1968) 30.
13. C. M. ADAM, in "Proceedings of Mechanical Behavior of Rapidly Solidified Materials", a symposium sponsored by the Mechanical Metallurgy Committee of ASM, AIME Annual Meeting, New York City, New York, 24–28 February 1985, edited by M. L. Sastry and A. MacDonald (AIME, New York, 1985) pp. 3,21.
14. M. H. BURDEN and H. JONES, *J. Inst. Metals* **98** (1970) 249.

Received 16 July 1990
and accepted 6 February 1991